Torsional Interaction Studies on a Power System Compensated by SSSC and Fixed Capacitor

G. N. Pillai, Arindam Ghosh, *Senior Member, IEEE*, and Avinash Joshi

***Abstract*—In this paper, a static synchronous series compensator (SSSC), along with a fixed capacitor, is used to avoid torsional mode instability in a series compensated transmission system. A 48-step harmonic neutralized inverter is used for the realization of the SSSC. The system under consideration is the IEEE first benchmark model on SSR analysis. The system stability is studied both through eigenvalue analysis and EMTDC/PSCAD simulation studies. It is shown that the combination of the SSSC and the fixed capacitor improves the synchronizing power coefficient. The presence of the fixed capacitor ensures increased damping of small signal oscillations. At higher levels of fixed capacitor compensation, a damping controller is required to stabilize the torsional modes of SSR.**

***Index Terms*—SSSC, torsional interaction, IEEE first benchmark model, eigenvalue analysis.**

I. Introduction

SERIES capacitors are widely used in long transmission lines to increase power transfer capability and improve transient stability. However, the extent to which a transmission line can be compensated with conventional series capacitor is often restricted by the need to avoid subsynchronous resonance (SSR). When devices based on power electronics known as flexible ac transmission system (FACTS) are introduced into a power system, a more flexible operation and control of transmission networks are obtained [1]. FACTS controllers can be classified as shunt, series, or phase angle compensating devices or devices which are a combination of the above three types. This paper concentrates on series compensation controllers. These controllers, in addition to realizing the conventional advantages of series compensation, have the potential to avoid or damp out SSR. Furthermore, these controllers would also enable fast control of the power transmitted on the line during transient power swings, thus allowing the transmission system to be safely operated much closer to its theoretical stability limit [1].

Advanced series compensator studies so far have mainly focussed on thyristor controlled series compensator (TCSC). However, TCSC suffers from some disadvantages [2]. It injects low order harmonic components (typically third, fifth, seventh, and ninth) into the power system because of phase control of thyristors. Transient response of the circuit is rather slow, because control of thyristor firing pulse is available only once in each half cycle. Deriving a closed-loop model of TCSC is complicated [3]. Other disadvantages include susceptibility to parallel resonance due to the presence of inductors and capacitors in parallel paths.

Static synchronous series compensator (SSSC) is implemented by a GTO-based voltage source inverter that can provide controllable compensating voltage over an identical capacitive and inductive range, independent of the magnitude of the line current [4]. Unlike other series compensators, an ideal SSSC is essentially a pure sinusoidal ac voltage source at the system fundamental frequency. Its output impedance at other frequencies is ideally zero. Thus, SSSC does not resonate with the inductive line impedance to initiate subsynchronous system oscillations. Fundamental principles, characteristics, and potential benefits of SSSC are described in [4]. Application of a 24-step SSSC for the control of power flow over a transmission line is given in [5]. Design, control, and application of a 48-step SSSC are presented in [6]. Performance of the SSSC in the IEEE First Benchmark Model is examined in [7]. In [7], it is shown that an increase in the conventional fixed series capacitor compensation increases the damping of small signal oscillations, whereas the SSSC maintains the damping level almost constant at a lower level. The effects of the value of the dc link capacitor of the SSSC on torsional modes are also studied in [7]. A robust controller based on H_∞ optimal control theory has been used to improve the torsional performance of SSSC [8].

This paper suggests that the SSSC be used as a constant synchronous voltage source in series with a fixed capacitor. This combination can be effective in avoiding subsynchronous oscillations that may be present in conventional fixed capacitor series compensation. Furthermore, this approach to series compensation results in an increased synchronizing power coefficient due to the fixed series capacitor and reduction of the MVAR rating of the SSSC. These factors, along with ease of power control, make the suggested configuration highly attractive for series compensation of transmission lines.

The SSSC consists of a 48-pulse voltage source converter (VSC), its magnetic circuit, and an interfacing transformer. In 48-pulse VSC, eight identical, elementary six-step inverters are operated from a common dc bus, each to produce a compatible set of three-phase, quasisquare wave output voltage waveforms. The magnetic circuit contains 18 single-phase three winding transformers and six single-phase two winding transformers [6], [7]. This connection eliminates all low-order harmonics. The lowest order harmonic on the ac side is 47th while that on the dc side is 48th.

Manuscript received June 13, 2001; revised May 13, 2002.
The authors are with the Department of Electrical Engineering, Indian Institute of Technology, Kanpur 208106, India.
Digital Object Identifier 10.1109/TPWRD.2003.813827

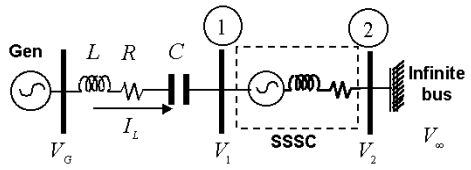

Fig. 1. Single-line diagram of an SSSC compensated power system.

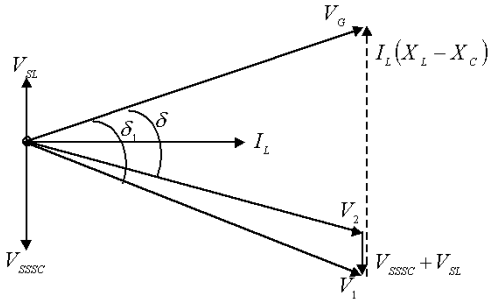

Fig. 2. Phasor diagram of SSSC compensated power system.

II. Improvement in Synchronizing Torque Coefficient

Fig. 1 shows an SSSC (between buses 1 and 2) and a fixed capacitor combination connected in series with a transmission line. The SSSC is represented by fundamental voltage source in series with an impedance. In the analysis presented below, variables given in uppercase letters denote phasor quantities, while the instantaneous quantities are given in lowercase letters.

Fig. 2 shows phasor diagram of the system indicating the voltage phasors V_G, V_1 and V_2 of generator bus and buses 1 and 2, respectively, and the line current phasor I_L. As an approximation, the small line and SSSC resistance voltage drops are neglected. $V_{\rm SL}$ indicates the leakage reactance drop in the SSSC system. The power flow between the generator and bus 1 is given by

$$P = \frac{V_G V_1}{(X_L - X_C)} \sin\delta_1$$

where $X_L = \omega L, X_C = 1/\omega C$ and δ_1 are shown in Fig. 2. Since both line and the SSSC are assumed to be lossless, the same power will flow through the SSSC as well. Assuming the generator voltage is regulated, the synchronizing power coefficient [9] is

$$\begin{aligned}\frac{\partial P}{\partial \delta} &= \frac{\partial P}{\partial \delta_1}\cdot\frac{\partial \delta_1}{\partial \delta} + \frac{\partial P}{\partial V_1}\cdot\frac{\partial V_1}{\partial \delta} \\ &= \frac{V_G V_1}{(X_L - X_C)}\cos\delta_1\left(\frac{\partial \delta_1}{\partial \delta}\right) \\ &\quad + \frac{V_G}{(X_L - X_C)}\sin\delta_1\frac{\partial V_1}{\partial \delta}\end{aligned}$$

where δ is also shown in Fig. 2. It can be shown that $\partial\delta_1/\partial\delta$ is close to unity, and $\partial V_1/\partial\delta$ is small and can be neglected. Thus, the increase in synchronizing power coefficient is decided by the reactance X_C of the fixed series capacitor in the line. When the compensator device is SSSC alone, effective impedance of the line is equal to the reactance of the transmission line.

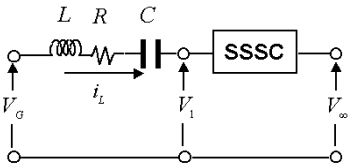

Fig. 3. Two-port network connected to infinite bus.

III. System Modeling for Eigenvalue Analysis

We shall now demonstrate the damping effects of SSSC through eigenvalue analysis. To do this, we have to develop a linear model of the overall system. The linearized models for the generator and shaft system for IEEE first benchmark model are well documented. Here, we use the approach given in [10].

A. Combined Generator and Shaft System Model

The linearized state equations are given by

$$\Delta\dot{x}_G = [A_G]\Delta x_G + [B_G]\Delta u_G \quad (1)$$

$$\Delta y_G = [C_G]\Delta x_G \quad (2)$$

where the state vector Δx_G, input vector Δu_G, and output vector Δy_G are given, respectively, by

$$\begin{aligned}\Delta x_G^T = [&\Delta\psi_d\ \Delta\psi_q\ \Delta E'_d\ \Delta E'_q\ \Delta\delta_g\ \Delta S_e\ \Delta T_{g,e}\ \Delta S_g \\ &\Delta T_{\rm LPB,g}\ \Delta S_{\rm LPB}\ \Delta T_{\rm LPA,LPB}\ \Delta S_{\rm LPA}\ \Delta T_{\rm IP,LPA} \\ &\Delta S_{\rm IP}\ \Delta T_{\rm HP,IP}\ \Delta S_{\rm HP}]\end{aligned}$$

$$\Delta u_G^T = [\Delta v_D \quad \Delta v_Q] \quad \text{and} \quad \Delta y_G^T = [\Delta i_{LD} \quad \Delta i_{LQ}].$$

In the equation just shown, the six mass mechanical system contains the generator (g), exciter (e), low pressure A (LPA), low pressure B (LPB), intermediate pressure (IP), and high pressure (HP) turbine shafts. The state variable ψ denotes the stator flux linkage, E' denotes the transient internal voltage, δ_g is the rotor angle, S denotes the per unit slip, and T denotes the torque. Note that the per unit slip S_i is defined as

$$S_i = (\omega_i - \omega_{\rm base})/\omega_{\rm base}$$

where $\omega_{\rm base}$ is 377 and ω_I is the speed of the ith shaft in electrical radians/s [10]. Therefore, ΔS_i represents the small signal change in the per unit shaft speed $\Delta(\omega_i/\omega_{\rm base})$. The torques between these shafts are indicated by subscripts. The vector Δu_G contains the terminal voltages and the vector Δy_G contains the armature currents. The generator electrical quantities are represented in d-q domain with respect to the synchronously rotating frame of the generator. The input and output quantities, however, are transformed with respect to a common reference D-Q frame for the entire system.

B. Network Model

The network shown in Fig. 3 can be split into two 2-port networks. The linearized equations for the first 2-port network consist of the transmission line and the fixed capacitor. These are given in D-Q domain [10] as

$$\Delta\dot{x}_{N1} = [A_{N1}]\Delta x_{N1} + [B_{N1}]\Delta y_G \quad (3)$$

$$\Delta u_G = \frac{X_L}{\omega}\Delta\dot{y}_G + [F_1]\Delta y_G + [F_{s1}]\Delta x_{N1} + \Delta e_1 \quad (4)$$

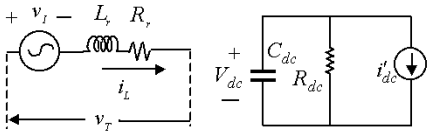

Fig. 4. SSSC equivalent circuit. (a) AC side. (b) DC side [6].

where

$$X_L = \omega L, \quad \Delta x_{N1}^T = [\,\Delta V_{cD} \quad \Delta V_{cQ}\,]$$
$$\Delta e_1^T = [\,\Delta V_{1D} \quad \Delta V_{1Q}\,] \quad A_{N1} = \begin{bmatrix} 0 & -\omega \\ \omega & 0 \end{bmatrix}$$
$$B_{N1} = \begin{bmatrix} \omega X_C & 0 \\ 0 & \omega X_C \end{bmatrix} \quad F_1 = \begin{bmatrix} R & X_L \\ -X_L & R \end{bmatrix},$$
$$F_{s1} = \begin{bmatrix} 1 & 0 \\ 0 & 1 \end{bmatrix}.$$

Note that the subscripts D and Q denote the D-Q components. The modeling of the other 2-port network is discussed below.

C. SSSC Model

The inverter configuration of SSSC used here consists of a 48-step inverter and magnetic circuit, which contains 18 single-phase three winding transformers and six single-phase two winding transformers [6], [7]. The ac and dc side equivalent circuits are shown in Fig. 4.

In Fig. 4(a), v_T is the voltage injected by SSSC. The series inductance L_r accounts for the leakage of the interfacing transformer and transformers in the magnetic structure of the inverter, while R_r represents the conduction losses of the inverter and transformer. In the dc side shown in Fig. 4(b), $V_{\rm dc}$ is the voltage across the dc capacitor that has a value of $C_{\rm dc}$, the resistance $R_{\rm dc}$ in shunt with the dc capacitor represents the switching losses, and $i_{\rm dc}$ is the current through the inverter as seen by the dc side.

The fundamental component of phase-a of the inverter output voltage is [6], [7]

$$v_{Ia} = \sigma \frac{16\sqrt{3}}{\pi} V_{\rm dc} \sin(\omega t + \theta_f) \tag{5}$$

where σ is the turns ratio of the interfacing transformer, ω is the fundamental frequency, and θ_f is the phase displacement of the inverter voltage with respect to reference bus.

Normalized per unit equations of the SSSC in DQ frame are [6]

$$\frac{d}{dt}\begin{bmatrix} i_{LD} \\ i_{LQ} \\ V_{\rm dc} \end{bmatrix} = \begin{bmatrix} -\frac{\omega R_r}{X_r} & -\omega & -\rho_1 \sin\theta_f \\ \omega & -\frac{\omega R_r}{X_r} & -\rho_1 \cos\theta_f \\ \rho_2 \sin\theta_f & \rho_2 \cos\theta_f & -\frac{\omega X_{\rm dc}}{R_{\rm dc}} \end{bmatrix} \begin{bmatrix} i_{LD} \\ i_{LQ} \\ V_{\rm dc} \end{bmatrix} + \begin{bmatrix} \frac{\omega}{X_r} & 0 & 0 \\ 0 & \frac{\omega}{X_r} & 0 \\ 0 & 0 & 1 \end{bmatrix} \begin{bmatrix} v_{TD} \\ v_{TQ} \\ 0 \end{bmatrix} \tag{6}$$

where $X_r = \omega L_r$, $X_{\rm dc} = (1/\omega C_{\rm dc})$, $\rho_1 = \sqrt{3}\omega/X_r$ $\rho_2 = \sqrt{3}\omega X_{\rm dc}$.

Linearizing (6), SSSC equations can be written as

$$\Delta \dot{x}_{N2} = [A_{N2}]\Delta x_{N2} + [B_{N2}]\Delta y_G + [B_C]\Delta\theta_f \tag{7}$$
$$\Delta v_1 = \frac{X_r}{\omega}\Delta \dot{y}_G + [F_2]\Delta y_G + [F_{s2}]\Delta x_{N2} + [F_C]\Delta\theta_f + \Delta e_2 \tag{8}$$

where

$$\Delta x_{N2} = \Delta V_{\rm dc}, \quad \Delta e_2^T = [\,\Delta v_{\alpha D} \quad \Delta v_{\alpha Q}\,]$$
$$[A_{N2}] = -\omega X_{\rm dc}/R_{\rm dc}$$
$$[B_{N2}] = \sqrt{3}\omega X_{\rm dc}[\,\sin\theta_{f0} \quad \cos\theta_{f0}\,]$$
$$[B_C] = \sqrt{3}\omega X_{\rm dc}(i_{Do}\cos\theta_{f0} - i_{Qo}\sin\theta_{f0})$$
$$F_2 = \begin{bmatrix} R_r & X_r \\ -X_r & R_r \end{bmatrix}$$
$$[F_{s2}]^T = [\,\sqrt{3}\sin\theta_{f0}, \quad \sqrt{3}\cos\theta_{f0}\,]$$

and

$$[F_c] = \sqrt{3}V_{\rm dco}(\cos\theta_{f0} - \sin\theta_{f0}).$$

Note that Δi_{LD} and Δi_{LQ} are contained in the vector Δy_G. These variables appear as input variables in (7) and (8). Therefore, state vector Δx_{N2} contains only the dc capacitor voltage $\Delta V_{\rm dc}$ Combining (3), (4), (7), and (8), the overall network model can be written as

$$\Delta \dot{x}_N = [A_N]\Delta x_N + [B_N]\Delta y_G + [B_C]\Delta\theta_f \tag{9}$$
$$\Delta u_G = \frac{X}{\omega}\Delta \dot{y}_G + [F]\Delta y_G + [F_s]\Delta x_N + [F_C]\Delta\theta_f + \Delta e_2 \tag{10}$$

where

$$[A_N] = \begin{bmatrix} A_{N1} & 0 \\ 0 & A_{N2} \end{bmatrix}, \quad [B_N]^T = [\,B_{N1} \quad B_{N2}\,],$$
$$[F] = [F_1] + [F_2], \quad [F_S] = [\,F_{s1} \quad F_{s2}\,]$$

and

$$X = X_L + X_r.$$

D. Combined System Model

Combining the generator and network models, we get the overall system equations

$$\dot{x} = Ax + Bu \tag{11}$$

where $x^T = [\Delta x_G \ \Delta x_N]$ and $u = \Delta\theta_f$

$$A = \begin{bmatrix} \left\{A_G + B_G H\left(FC_G + \frac{X_T}{\omega_B}C_G A_G\right)\right\} & B_G H F_s \\ B_N C_G & A_N \end{bmatrix}$$

$$B^T = [\,B_G H F_C \quad B_C\,] \quad \text{and} \quad H = \left\{I - \frac{X_T}{\omega}[C_G][B_G]\right\}^{-1}.$$

IV. System Studies

The system considered is the IEEE first benchmark model for SSR analysis [11]. This system is characterized by four unstable torsional modes that are distributed in a relatively wide

TABLE I
EIGENVALUES OF COMPENSATED SYSTEM

Modes	Capacitor 0.3 pu	Capacitor+SSSC 0.15+0.15 pu	Capacitor+SSSC 0.2+0.15 pu	Capacitor+SSSC 0.3+0.15 pu
Super synchr.	-4.462 ± j 594.96	-5.461 ± j537.27	-5.58 ± j560.35	-5.27 ± j599.16
Sub synchr.1	-4.727 ± j159.12	-5.916 ± j246.07	-6.33 ± j 225.61	-7.44 ± j193.85
Sub synchr.2	*	-5.047 ± j74.74	-4.61 ± j 72.44	-3.54 ± j66.45
Mode 0	-1.06 ± j9.19	-0.781 ±j8.76	-0.82 ± j9.30	-1.02 ± j10.60
Mode 1	-0.131 ± j99.41	-0.261 ± j98.63	-0.28 ± j98.63	-0.31 ± j98.63
Mode 2	-0 .646 ± j127.07	-0.664± j127.0	-0.665 ± j127.01	-0.67 ± j127.01
Mode 3	1.02 ± j160.16	-0.1836±j160.56	-0.19 ± j160.57	-0.191 ± j160.6
Mode 4	-0.034 ± j202.74	-0.0627±j202.95	-0.059 ± j203.03	0.19 ± j202.74
Mode 5	-0.182 ± j 298.18	-0.182 ± j 298.18	-0.182 ± j298.18	-0.18 ± j298.18

frequency range. A steady-state operating point is chosen in which the machine operates with a power factor of 0.9 while delivering a power of 0.7 p.u. Self-damping of 0.1 is added to the shaft. No mutual damping is assumed. Constant field voltage is also assumed. Infinite bus voltage is 481.33 kV.

A. System Response With a PI Controller

Taking the state variable $\Delta V_{\rm dc}$ as the output, the output equation can be written as

$$y = [0\,0 \ldots 0\,1] \quad x = H\,x. \tag{12}$$

We now choose a proportional-plus-integral (PI) controller to compensate for any variation in $\Delta V_{\rm dc}$ [6]. The control law in Laplace-domain is then given by

$$\Delta\theta_f = \left(K_p + \frac{K_i}{S}\right)(\Delta V_{\rm dcref} - \Delta V_{\rm dc}). \tag{13}$$

Since the dc capacitor voltage is held constant, $V_{\rm dcref}$ in the above equation will be zero. We now combine (11)–(13) to obtain a homogeneous state space equation that can be used for eigenvalue analysis. A proportional gain (K_p) of 1.0 and an integral gain (K_i) of 500 is chosen as the controller parameters. The SSSC parameters are given in [7]. The value of dc capacitance chosen based on the guidelines in [7] is 3000 μF.

Below, we compare the results of a fixed capacitor compensated line with those of three different combinations of fixed capacitor and SSSC. In all of the three combinations, it is assumed that the SSSC is providing 0.15-p.u. compensation. The eigenvalues of four cases are listed in Table I.

With a fixed capacitor of 0.3 p.u., the torsional mode 3 is unstable. It can be seen that the oscillation frequency of the subsynchronous electrical mode approaches frequency of torsional mode 3 at this compensation level. When the fixed capacitor-SSSC combination is used with a capacitor value of 0.15 p.u., all of the torsional modes become stable. It can be seen from Table I that the damping of the 0th mode increases with the value of fixed capacitor and so does the synchronizing power coefficient (imaginary part of the 0th mode). Furthermore, when the value of the fixed capacitor is large, the system gets destabilized despite the presence of the SSSC. This is evident from column 4 of Table I in which the torsional mode 4 is unstable. Results of the eigenvalue analysis are validated through PSCAD/EMTDC simulation. In practice, it is not feasible to measure the firing angle with respect the infinite bus. Thus a local bus between the generator and SSSC is chosen for setting the angle reference. This had the added advantage that the control system requires only the local measurements. The firing angle of the SSSC with respect to the local bus 1 in Fig. 1 is 93.45° (lagging).

A bolted, three-cycle, three-phase to ground fault is created between the SSSC and the infinite bus when the system is operating in steady state for 0.5 s. System responses are shown in Fig. 5. The response of the system, when the compensation is provided only by a fixed capacitor, is shown in Fig. 5(a). The system is unstable under the influence of torsional interaction (mode 3). The results of Fig. 5(b) are shown for the fixed capacitor-SSSC combination when each of them is providing a compensation of 0.15 p.u. (column 2 of Table I). It is evident from this figure that the system has now been stabilized. Fig. 5(c) depicts magnified version of the LPA-LPB torque corresponding to the one shown in Fig. 5(a). It can be seen that the frequency of this unstable mode 3 is approximately 160 rad/s or 25 Hz. Fig. 6 shows line current, dc capacitor voltage, injected voltage, and the firing angle of the SSSC with respect to the local bus.

B. System Response With a Damping Controller

The results presented before show that when high values of fixed compensation are used along with SSSC, torsional modes become unstable. Damping of the torsional modes can be increased by an auxiliary controller which modulates the output of the PI controller. Fig. 7 shows the block diagram of the controller, in which the auxiliary signal ΔS_g is the small signal

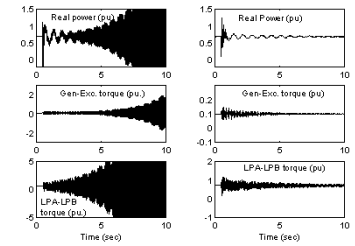

(a) (b)

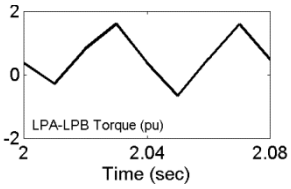

(c)

Fig. 5. System response to bolted three-phase fault in (a) fixed capacitor, (b) capacitor plus SSSC compensated power system, and (c) magnified LPA-LPB torque of (a).

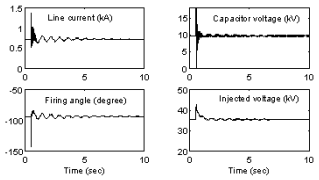

Fig. 6. Line current, dc capacitor voltage, injected voltage, and firing angle of SSSC.

change in per unit generator speed. The output vector in state (12) will become

$$y^T = [\,\Delta V_{\rm dc} \quad \Delta S_g\,].$$

Taking the Laplace transform of (11) and (12), we have the state equations in frequency domain

$$\left.\begin{aligned} sx(s) &= Ax(s) + Bu(s) \\ y(s) &= Hx(s) \end{aligned}\right\}. \tag{14}$$

The input signal in this case has two parts. This is given by

$$\begin{aligned} u(s) &= G_1(s)\Delta V_{\rm dc}(s) + G_2\Delta S_g(s) \\ &= G(s)y(s) \end{aligned} \tag{15}$$

where $G(s) = [G_1(s)\, G_2(s)]$, $G_1(s)$ being the transfer function of the PI controller and $G_2(s)$ is given by

$$G_2(s) = \frac{KT_w s}{1+sT_w}\frac{(1+sT_1)}{(1+sT_2)}\frac{(1+sT_3)}{(1+sT_4)}.$$

$G_2(s)$ consists of a wash out block and a second order lead compensator whose parameters are selected to provide damping at higher (torsional) frequencies. Combining (14) and (15), we get a homogeneous state space equation of the form

$$sx(s) = [A + BG(s)H]x(s).$$

Then, the characteristic equation of the closed loop system is given by

$$|sI - (A + BG(s)H| = 0. \tag{16}$$

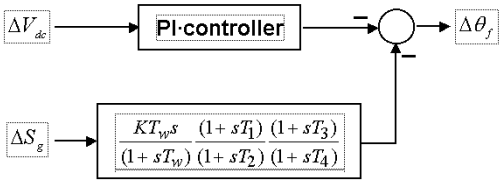

Fig. 7. Block diagram of the SSSC PI and damping controllers.

TABLE II
TORSIONAL MODES WITH DAMPING CONTROLLER

Mode Number	Eigenvalues
0	-1.19 ± j10.9
1	-0.45 ± j97.7
2	-0.68 ± j126.9
3	-0.39 ± j160.2
4	-0.26 ± j204.7
5	-0.8 ± j298.2

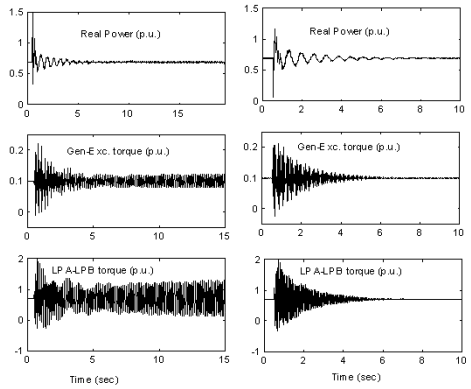

(a) (b)

Fig. 8. System response to large signal fault in capacitor plus SSSC ($0.3+0.15$ p.u.) compensated system. (a) Without damping controller. (b) With damping controller.

The parameters of the damping controller are chosen as

$$K = 1, \quad T_w = 10, \quad T_1 = 0.2, \quad T_2 = 0.001,$$
$$T_3 = 0.1, \quad T_4 = 0.001.$$

Table II shows the critical eigenvalues of the closed loop system when damping controller is used. Without the damping controller, when fixed capacitor compensation level is 0.3 p.u. and SSSC compensation level is 0.15 p.u., the torsional mode 4 is unstable (Table I). When damping controller is used, it is obvious from the table that the damping for all torsional modes is increased.

In order to illustrate the effectiveness of the damping controller, nonlinear time domain simulation is performed as before and results are shown in Fig. 8. In this, Fig. 8(a) shows the system performance when the damping controller is not used. In accordance with the 4th column of Table I, the system is unstable as the oscillations in the LPA-LPB mode are growing. The

system is stabilized with the damping controller. This is evident from Fig. 8(b).

V. Conclusion

Addition of an SSSC in a series compensated power system provides superior performance characteristics and application flexibility not achievable by conventional series capacitors. The voltage source nature of the SSSC can stabilize the unstable torsional modes of a fixed capacitor compensated transmission system as it increases the damping of the torsional and network modes. The presence of series capacitor increases the synchronizing power coefficient. It also improves the small signal stability of power system. Reduction of the MVAR rating of the SSSC is an added advantage of the combination. High values of capacitive reactance can cause torsional interaction. An auxiliary controller that modulates the output of the PI controller can stabilize the torsional modes. Thus, with the combination of the SSSC and damping controller, the amount of fixed compensation can be increased without endangering the system stability.

References

[1] "Flexible AC Transmission Systems (FACTS)," Electrical Power Research Institute Rep., Number EL-6943, Sept. 1991.

[2] K.-H. Chu and C. Pollock, "PWM-controlled series compensation with low harmonic distortion," in *Proc. Inst. Elect. Eng.—Gen., Transm. Dist.*, vol. 144, 1997, pp. 555–560.

[3] A. Ghosh and G. Ledwich, "Modeling and control of thyristor-controlled series compensators," in *Proc. Inst. Elect. Eng.-Gen., Transm. Dist.*, vol. 142, 1995, pp. 297–304.

[4] L. Gyugyi, C. D. Schauder, and K. K. Sen, "Static synchronous series compensator: A solid-state approach to the series compensation of transmission lines," *IEEE Trans. Power Delivery*, vol. 12, pp. 406–417, Jan. 1997.

[5] K. K. Sen, "SSSC—Static synchronous series compensator: Theory, modeling and application," *IEEE Trans. Power Delivery*, vol. 13, pp. 241–246, Jan. 1998.

[6] L. S. Kumar and A. Ghosh, "Modeling and control design of a static synchronous series compensator," *IEEE Trans. Power Delivery*, vol. 14, pp. 1448–1453, Oct. 1999.

[7] G. N. Pillai, A. Ghosh, and A. Joshi, "Torsional oscillation studies in an SSSC compensated power system," *Elect. Power Syst. Res.*, vol. 55, pp. 57–64, 2000.

[8] ——, "Robust control of SSSC to improve torsional damping," in *IEEE Power Eng. Soc. Winter Meeting*, Columbus, OH, Jan./Feb. 2001.

[9] P. M. Anderson and A. A. Fouad, *Power System Control and Stability*. Ames, IA: The Iowa State Univ. Press, 1977.

[10] K. R. Padiyar, *Power System Dynamics: Stability and Control*. Bangalore, India: Interline, 1996.

[11] IEEE SSR Task Force of the Dynamic System Performance Working Group, Power Syst. Eng. Committee, "First benchmark model for computer simulation of subsynchronous resonance," *IEEE Trans. Power Apparat. Syst.*, vol. PAS-96, pp. 1565–1571, 1977.

G. N. Pillai received the M.Tech. degree from Regional Engineering College, Kurukshetra, India, in 1989, and the Ph.D. degree from Indian Institute of Technology (IIT), Kanpur, India, in December 2001.

Currently, he is Faculty Member in Electrical Engineering Department in the Regional Engineering College Kurukshetra since 1989. His interests are in the areas of power systems and controls.

Arindam Ghosh (S'80–M'83–SM'93) received the Ph.D. degree in electrical engineering from the University of Calgary, AB, Canada, in 1983.

Currently, he is a Professor of Electrical Engineering at Indian Institute of Technology (IIT), Kanpur, India, where he has been since 1991. He has held visiting positions with Nanyang Technological University, Singapore, and with the University of Queensland and Queensland University of Technology, Australia. His interests are in control of power systems and power electronic devices.

Avinash Joshi received the Ph.D. degree in electrical engineering from the University of Toronto, ON, Canada, in 1979.

Currently, he is a Professor of Electrical Engineering at the Indian Institute of Technology, Kanpur. He worked at the G.E.C. of India Ltd., Calcutta, India, from 1970 to 1973. His interests include power electronics circuits, digital electronics, and microprocessor systems.